

SUPPLEMENTARY MATERIAL

Nitrogen-doped hollow carbon spheres as chemical vapour sensors

Bridget K. Mutuma^{ac*}, Clara I. Garcia-Martinez^b, Rodrigo C. Dias^b, Boitumelo J. Matsoso^{ad}, Neil J. Coville^a,
and Ivo A. Hümmelgen^{b,e}

^a DST-NRF Centre of Excellence in Strong Materials and the Molecular Sciences Institute, School of Chemistry, University of the Witwatersrand, WITS 2050, Johannesburg, South Africa.

^b Departamento de Física, Universidade Federal do Parana, Caixa Postal 19044, 8153-980 Curitiba, PR, Brazil. E-mail:

^c Department of Physics, Institute of Applied Materials, University of Pretoria, 0028, Pretoria, South Africa. E-mail:

bridgetmutuma@gmail.com; Tel: +2712-420-6780

^d Laboratoire des Multimatériaux et Interfaces, UMR-5615 CNRS, Université Claude Bernard Lyon 1, Villeurbanne-Cedex

^e Deceased

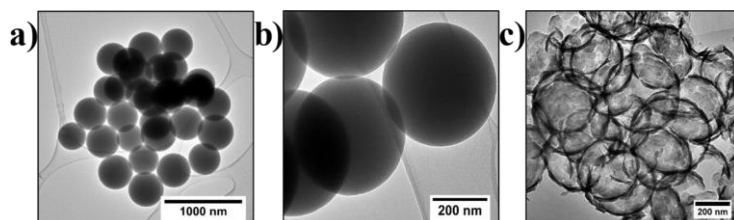


Figure S1: TEM images of; (a-b) SiO₂ spheres and (b) N-HCSs-50.

Figure S2b inset shows the pore size distribution calculated by the Barrett-Joyner-Halenda (BJH) method with a broad peaks observed between 20 and 100 nm for all the HCSs; characteristic of the presence of pores and voids in the mesoporous and macroporous region¹. In the N-HCSs-50, a sharp peak was observed at 100 nm indicating the creation of macropores probably resulting from void of the broken HCSs.

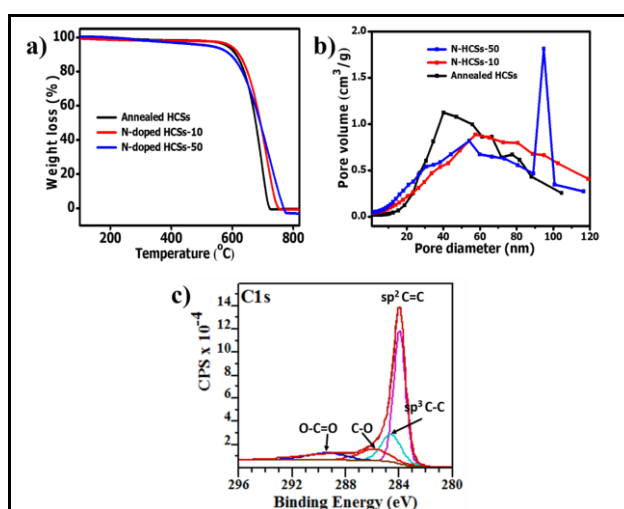


Figure S2: Thermal gravimetric curves, (b) pore size distribution plots of annealed HCSs and N-HCSs and (c) C 1s spectra of annealed HCSs.

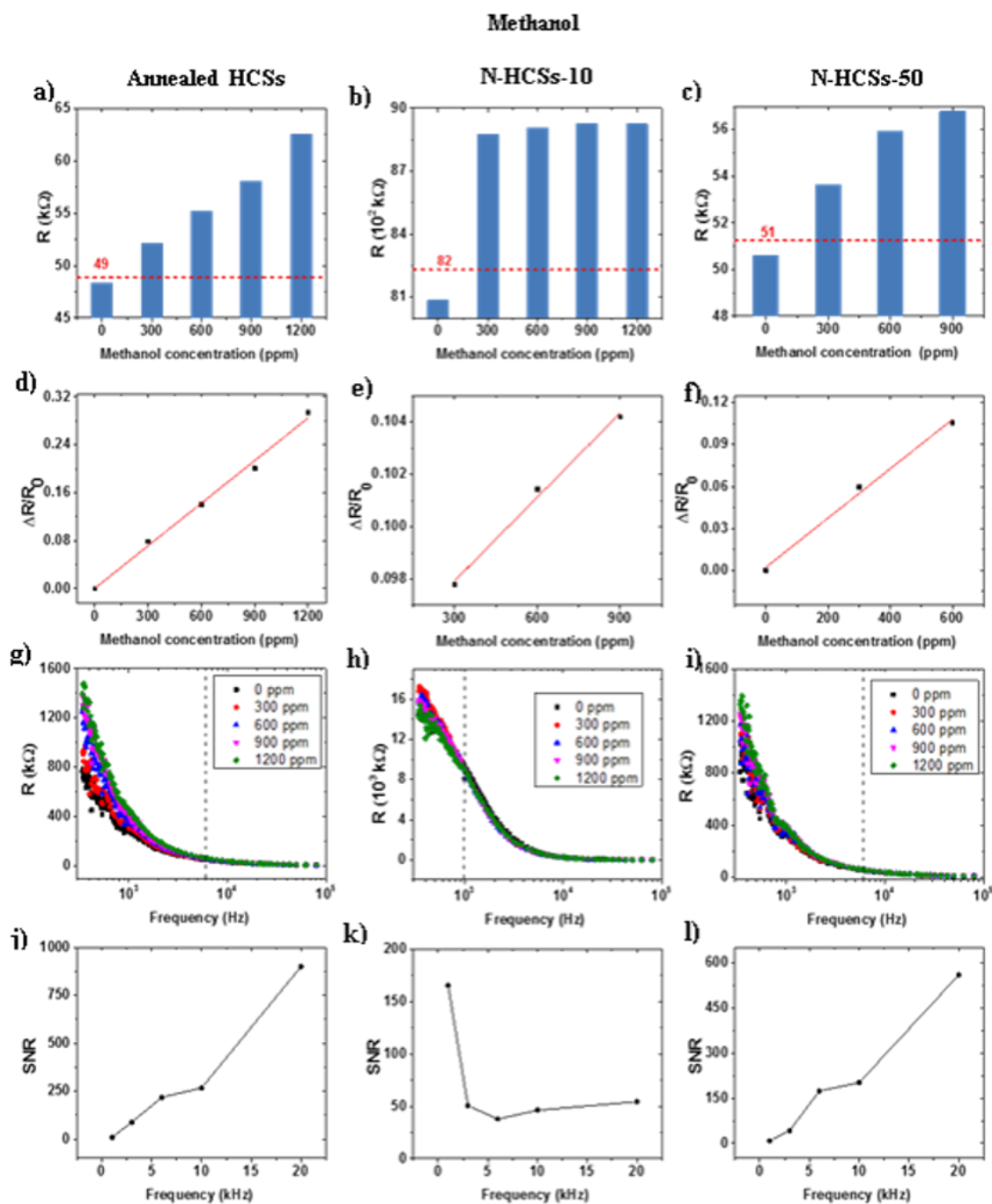


Figure S3: (a-c) Sensor resistance as a function of analyte (methanol) concentration, the red line indicates the estimated LoD resistance of the corresponding sensor; (d-f) response of the sensor versus analyte concentration; (g-i) sensor resistance dependence on frequency, dashed line indicates the optimum operating frequency and (j-l) sensor signal to noise ratio as a function of frequency. Corresponding results based on annealed HCSs, N-HCSs-10 and N-HCSs-50 are presented in the first, second and third column, respectively.

Toluene

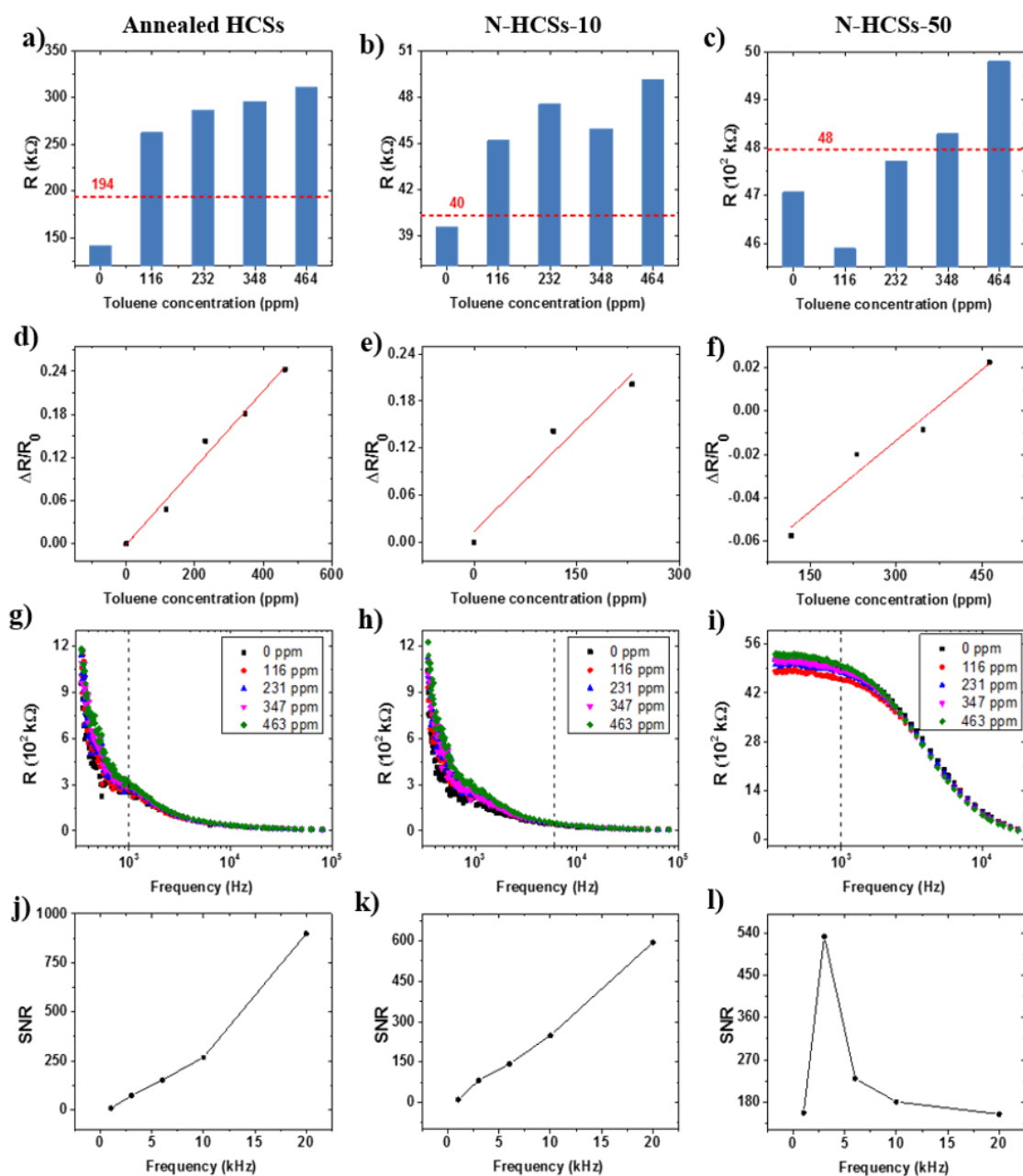


Figure S4: (a-c) Sensor resistance as a function of analyte (toluene) concentration, the red line indicates the estimated *LoD* resistance of the corresponding sensor; (d-f) response of the sensor versus analyte concentration; (g-i) sensor resistance dependence on frequency, dashed line indicates the optimum operating frequency and (j-l) sensor signal to noise ratio as a function of frequency. Corresponding results based on annealed HCSs, N-HCSs-10 and N-HCSs-50 are presented in the first, second and third column, respectively.

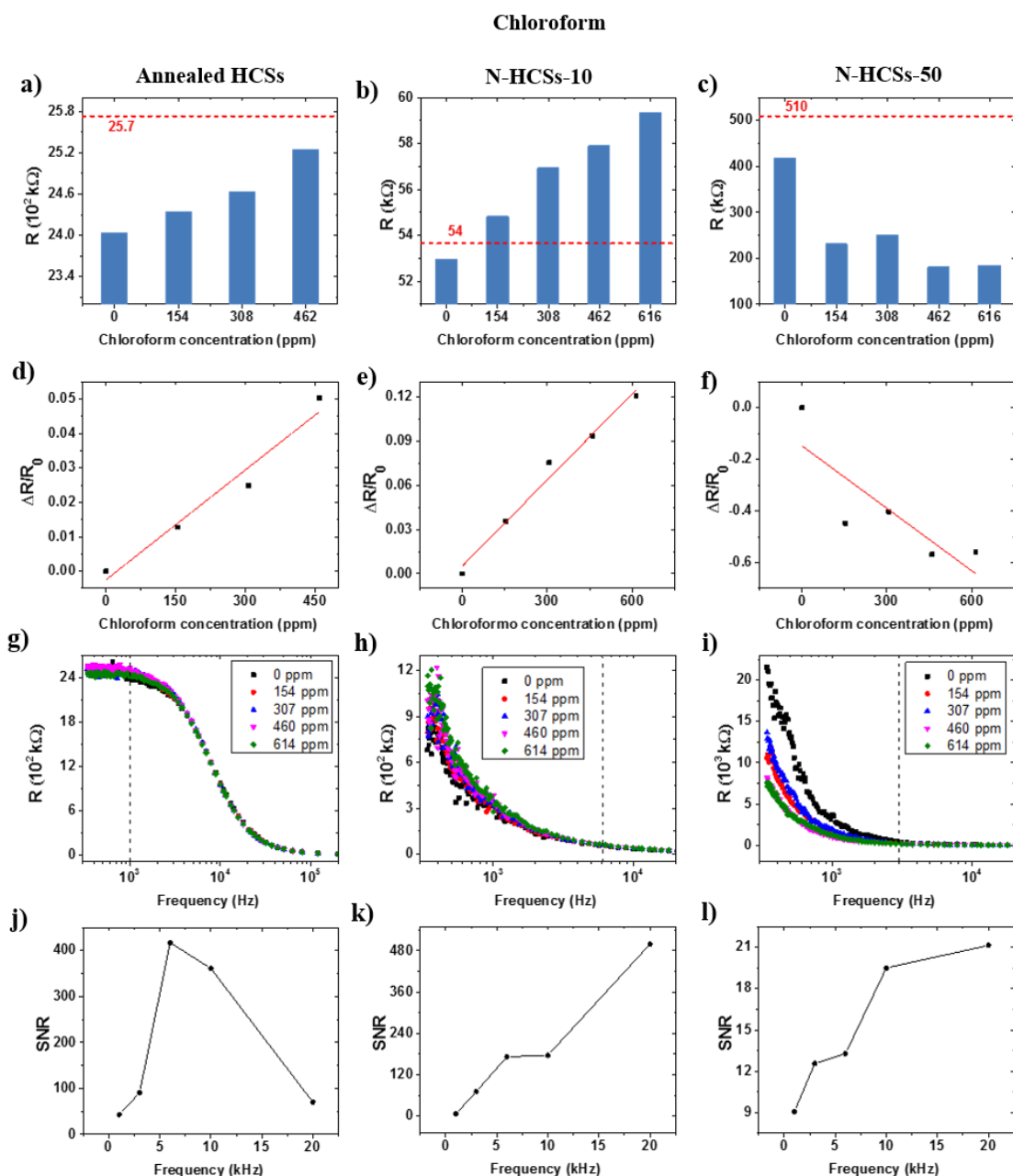


Figure S5: (a-c) Sensor resistance as a function of analyte (chloroform) concentration, the red line indicates the estimated *LoD* resistance of the corresponding sensor; (d-f) response of the sensor versus analyte concentration; (g-i) sensor resistance dependence on frequency, dashed line indicates the optimum operating frequency and (j-l) sensor signal to noise ratio as a function of frequency. Corresponding results based on annealed HCSs, N-HCSs-10 and N-HCSs-50 are presented in the first, second and third column, respectively.

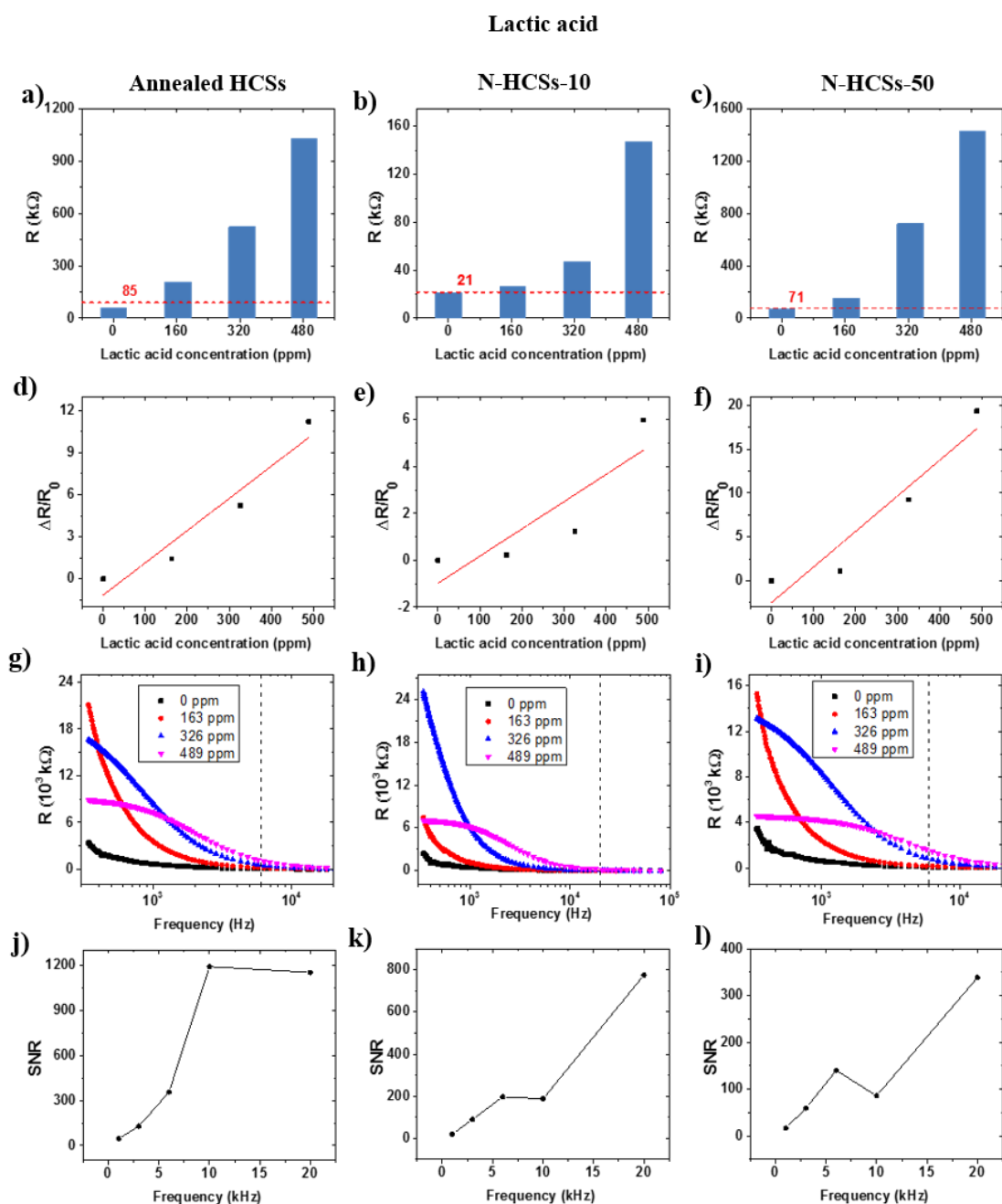


Figure S6: (a-c) Sensor resistance as a function of analyte (lactic acid) concentration, the red line indicates the estimated LoD resistance of the corresponding sensor; (d-f) response of the sensor versus analyte concentration; (g-i) sensor resistance dependence on frequency, dashed line indicates the optimum operating frequency and (j-l) sensor signal to noise ratio as a function of frequency. Corresponding results based on annealed HCSs, N-HCSs-10 and N-HCSs-50 are presented in the first, second and third column, respectively.

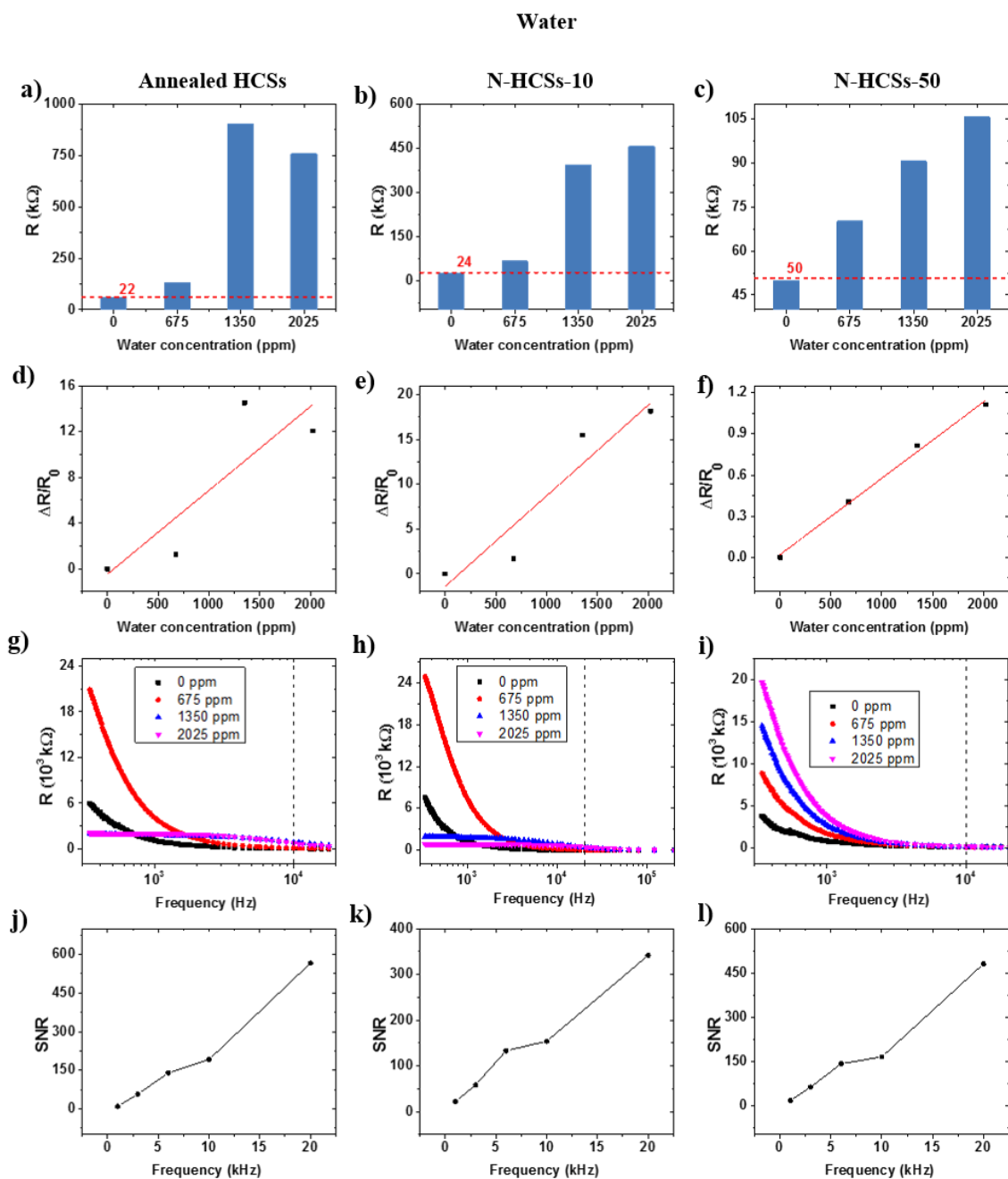


Figure S7: (a-c) Sensor resistance as a function of analyte (water) concentration, the red line indicates the estimated LoD resistance of the corresponding sensor; (d-f) response of the sensor versus analyte concentration; (g-i) sensor resistance dependence on frequency, dashed line indicates the optimum operating frequency and (j-l) sensor signal to noise ratio as a function of frequency. Corresponding results based on annealed HCSs, N-HCSs-10 and N-HCSs-50 are presented in the first, second and third column, respectively.

Acetone

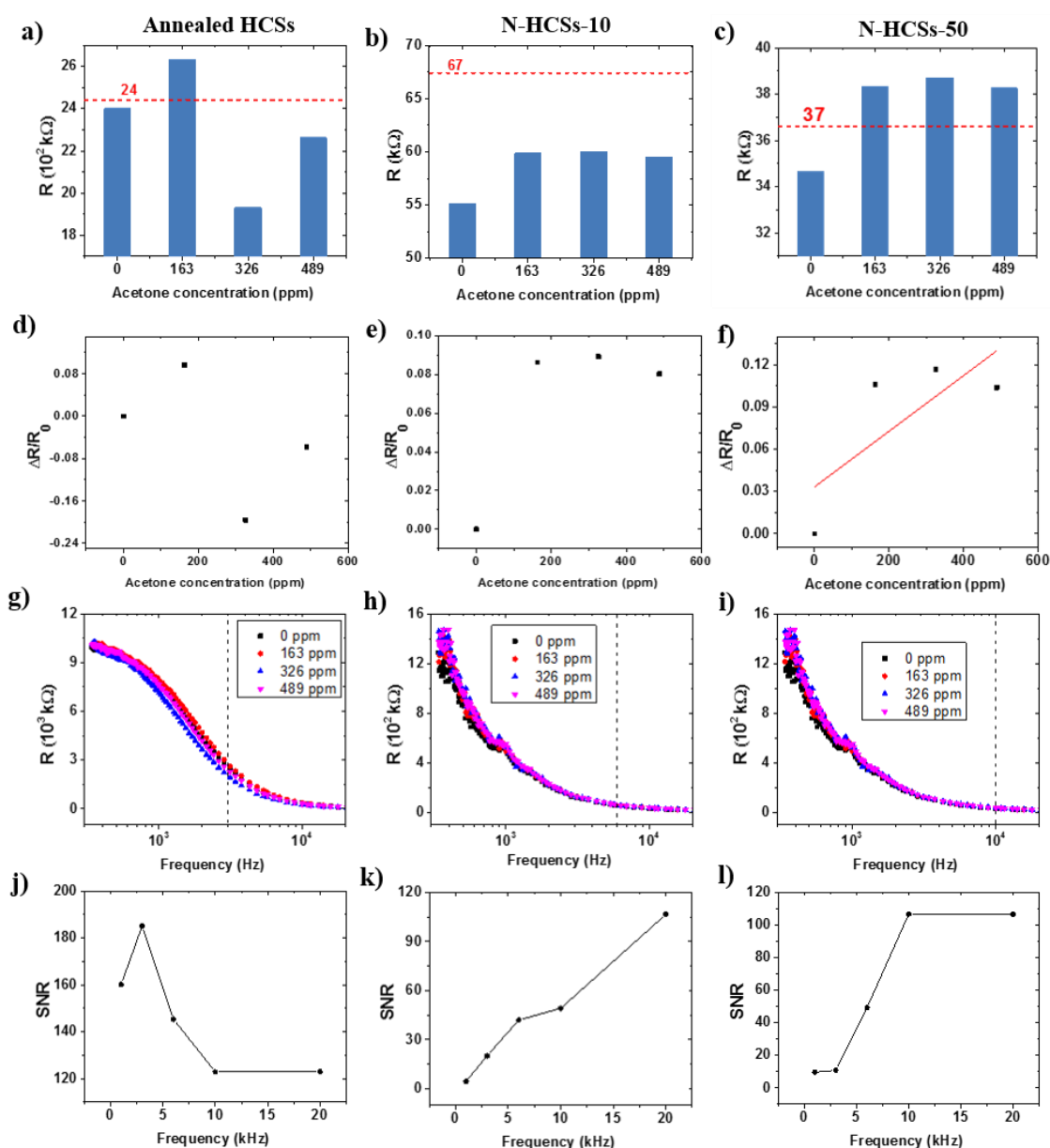


Figure S8: (a-c) Sensor resistance as a function of analyte (acetone) concentration, the red line indicates the estimated LoD resistance of the corresponding sensor; (d-f) response of the sensor versus analyte concentration; (g-i) sensor resistance dependence on frequency, dashed line indicates the optimum operating frequency and (j-l) sensor signal to noise ratio as a function of frequency. Corresponding results based on annealed HCSs, N-HCSs-10 and N-HCSs-50 are presented in the first, second and third column, respectively.

References

- 1 M. Thommes, *Chemie Ing. Tech.*, 2010, **82**, 1059–1073.